RSC Advances

REVIEW

View Article Online
View Journal | View Issue

Cite this: *RSC Adv.*, 2020, **10**, 30094

Rational design of yolk–shell nanostructures for drug delivery

Ghodsi Mohammadi Ziarani, *[a] Parisa Mofatehnia,[a] Fatemeh Mohajer[a] and Alireza Badiei[b]

Yolk–shell nanoparticles (YSNPs) are a new class of hollow nanostructures, and their unique properties can be utilized in drug delivery systems. The recent progress in YSNPs-based carriers is highlighted in drug delivery systems. Doxorubicin hydrochloride, ceftriaxone sodium, and methotrexate are three of the most common drugs that are used in this field. According to the reported studies, the materials used most often as yolk–shells are magnetic nanoparticles and polymers. The used methods for synthesizing a diverse array of YSNPs are classified based on their core structures. Various properties of YSNPs include their high drug-loading capacity, and their ability to decrease drug toxicity and satisfactorily and efficiently release drugs.

Received 22nd April 2020
Accepted 28th July 2020

DOI: 10.1039/d0ra03611k

rsc.li/rsc-advances

1. Introduction

The desired behavior of *in vivo* nanomedicine is dependent upon the physicochemical properties of the drug carrier, such as size, shape, elasticity, surface charge, and functionalization. Also, the creation of novel drug carrier structures with inorganic and organic materials can yield new drug delivery systems.[1] Many chemotherapy drugs have toxic effects, but their encapsulation reduces their side effects before reaching the target. Inorganic encapsulation materials such as organic polymers, liposomes, silica, and bioceramics have been used.[2,3] Yolk–shell structures or so-called nano-rattles are a particular class of core–shell configuration with a unique core@void@shell that have been widely used due to their catalysis ability,[4–7] and have been applied as nanoreactors,[8,9] and in energy storage[10] and drug delivery systems.[11] A wide range of chemical compositions, including NPs@silica, metal oxide@silica,[12] metal NPs@carbon,[13] metal NPs@metal oxide,[14]

[a]*Department of Chemistry, Faculty of Physics and Chemistry, University of Alzahra, Tehran, Iran. E-mail: gmohammadi@alzahra.ac.ir; Fax: +98 21 88613937; Tel: +98 21 88613937*

[b]*School of Chemistry, College of Science, University of Tehran, Tehran, Iran*

Ghodsi Mohammadi Ziarani received her B. Sc. degree in Chemistry from Teacher Training University, Tehran, Iran, in 1987, her M. Sc. degree in Organic Chemistry from the Teacher Training University, Tehran, Iran, under the supervision of Professor Jafar Asgarin and Professor Mohammad Ali Bigdeli in 1991 and her Ph. D. degree in asymmetric synthesis (biotransformation) from Laval University, Quebec, Canada under the supervision of Professor Chenevert, in 2000. She is a Full Professor of Organic Chemistry in the chemistry department of Alzahra University. Her research interests include organic synthesis, heterocyclic synthesis, asymmetric synthesis, natural products synthesis, synthetic methodology and applications of nano-heterogeneous catalysts in multicomponent reactions.

Parisa Mofatehnia was born in 1991 in Yasuj, Iran. She received her B. Sc. degree in Pure Chemistry at Yasuj University (2014). In the same year, she was accepted for an M. Sc. degree in Organic Chemistry at Yasuj University. Parisa started her M. Sc. thesis under the supervision of Dr Dawood Elhamifar on the application of catalysts in organic reactions. She is currently a Ph. D. candidate in Organic Chemistry at Alzahra University under the supervision of Prof. Ghodsi Mohammadi Ziarani.

metal NPs@polymer, silica@metal oxide, silica@carbon,[15] and polymer@polymer[16] have been used in these structures, which are widely applied in drug delivery systems. They contain movable cores, porous shells, hollow interiors, controllable sizes and shapes, and large voids. YSNPs contain an ample hollow space between the core and shell that is particularly suitable for loading with fluorescent or drug molecules.[17–20]

This review reports an overview of the synthetic methods, biological properties, and potential applications of yolk–shell nanoparticles (YSNPs) in drug delivery systems. Several methods have been reported for preparing YSNPs: the Kirkendall diffusion method.[21–23] ripening method,[24] hard template method,[15,25,26] soft template assembly,[27] the ship-in-bottle,[28,29] and hydrothermal and solvothermal methods.[30] YSNPs are commonly classified by morphology into six groups: single-core@single-shell, multiplecores@single-shell, void@single-shell, single-core@multiple-shells, multiple-cores@multiple-shells, and void@multiple-shells.[31] Additionally, due to the importance of the core in their structures, considerable use has been made of organic and inorganic core-based yolk/shell structures in recent years. In continuation of our reviews on the synthesis of different natural products[32–34] and the application of different support in drug deliveries[35–37], a new category based on the core of YSNPs is disclosed in this review.

2. The synthesis of silica-based yolk–shell nanostructures (SYSNs)

Silica-based yolk–shell nanostructures (SYSNs) are synthesized by a green and straightforward route, as shown in Scheme 1. The silica nanosphere core is synthesized by a modified Stöber method, and then it is coated through two surfactants involving cetyltrimethyl ammonium bromide (CTAB) and dodecanol as a soft co-template. Then, tetraethyl orthosilicate (TEOS) is added to the previous solution, resulting in two layers of silica with different degrees of porosity that are composed to prepare silica core–shell–shell nanospheres (CSSNs). They are subsequently transformed into SYSNs by modification with fluorescein isothiocyanate (FITC) and polyethylene glycol (PEG) as shown in Scheme 2.[38,39] Doxorubicin hydrochloride (DOX) is loaded onto SYSNs and effectively could be used to treat breast cancer cells without highly toxic side effects.

2.1. The synthesis of the yolk–shell structure with a mesoporous shell

Mesoporous yolk–shell structures have different cores, including silica nanospheres,[40] SiO_2–Au, Mobil Composition of Matter No. 41 (MCM41) mesoporous,[41] Institute of Bioengineering and Nanotechnology 1 (IBN1) mesoporous,[42] IBN4 mesoporous,[42] Santa Barbara Amorphous-15 (SBA-15),[43] magnetic Fe_3O_4/silica composites,[44] and Au nanoparticles.[45] To prepare the shell, a solution of water, ethanol, fluorocarbon surfactant (FC4), triblock copolymer EO106PO70EO106 (F127), and aqueous ammonia was added to the aqueous solution of the core material, and the solution was then stirred for a certain amount of time. Then, TEOS was added to the mixture, which was eventually heated for a certain amount of time for hydrolysis and condensation in a Teflon-lined autoclave. In the next step, the dry composite silica powder was further calcined at 550 °C to remove the organic templates (Scheme 3).[46] These particular mesoporous yolk–shell structures are capable of a the three-step release of drugs. The yolk–shell materials can be used for developing nanoreactors as drug or gene delivery vehicles.

2.2. The synthesis of amorphous calcium phosphate (ACP) nanospheres with a yolk–shell structure

Amorphous calcium phosphate (ACP) nanospheres with a yolk–shell structure can be prepared by combining three solutions consisting of phenol-formaldehyde resin spheres (PRs), P_2O_5, and $Ca(NO_3)_2 \cdot 4H_2O$ with anhydrous ethanol, and the resultant powder was heated to 500 °C for calcination. Finally, the yolk@cage–shell hollow mesoporous mono-dispersion nanospheres of ACP were successfully constructed.[47] DOX was loaded into the yolk@cage–shell hollow ACP nanospheres. The difference in DOX absorption behavior may be different in various morphologies. For our

Fatemeh Mohajer was born in Tehran, Iran and she received her B. Sc. in Applied Chemistry from Bu-Ali Sina University and M. Sc degree in Organic Chemistry from Azad University in Karaj. She is a Ph. D student under the supervision of Prof. Ghodsi Mohammadi Ziarani at Alzahra University in Tehran, Iran.

Alireza Badiei was born in Iran, in 1965. He received his B. Sc and M. Sc degrees in Chemistry and Inorganic Chemistry from the Teacher Training University (Kharazmi), Tehran, Iran, in 1988 and 1991, respectively, and his Ph. D degree in the synthesis and modification of nanoporous materials from Laval University, Quebec, Canada, in 2000. He is currently a full Professor in the Chemistry faculty of Tehran University. His research interests include nanoporous materials synthesis, modification of nanoporous materials and application of organic–inorganic hybrid materials in various fields such as catalysis, adsorption, separation and sensors.

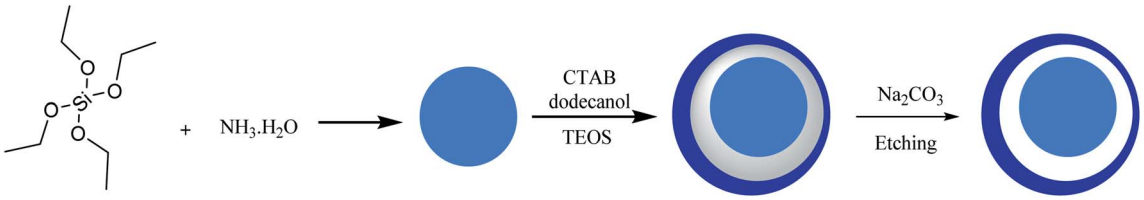

Scheme 1 The synthesis of CSSN and SYSNs.

investigation, we planned that DOX would be absorbed on a different ACP morphology, and thus, a spherical hollow particle (Scheme 4a) and a single-layer hollow spherical cage-like ACP nanoparticle without a yolk (Scheme 4b) were also synthesized. The yolk@cage–shell with hollow structure nanospheres, large pore size, and larger interior space exhibited a greater loading capacity than hollow ACP and cage-like ACP nanoparticles (Scheme 4c). The loading capacity for DOX molecules was 1181.9 mg g^{-1}, which was due to the large pore sizes and interior space.

3. Synthesis and application of metal yolk-based yolk–shell structures

3.1. The synthesis of yolk–shell porous iron oxide@magnesium silicate nanospheres

Iron oxide@magnesium silicate yolk–shell porous nanospheres were synthesized with superparamagnetic properties. This synthesis procedure consists of three steps. First, the superparamagnetic iron oxide was prepared and modified by TEOS to make superparamagnetic iron oxide@SiO_2. In the next level, the magnesium silicate shell was produced by a solvothermal technique and adding SPIO@SiO_2 powder to a solution containing magnesium and acetate ions. The creation of a bond between silicate ions and magnesium produced magnesium–silicate nanosheets as the final stage (Scheme 5).[48] Anticancer drug DOX was selected as a model, which was also investigated under both *in vivo* and *in vitro* conditions through the implantation of the drug on the yolk–shell bed. Then, the drug-releasing test was performed under *in vitro* conditions. An increased rate of drug release indicates the high efficiency of superparamagnetic yolk–shell porous nanospheres. Thus, prepared yolk–shell porous nanospheres of SPIO@MS are promising for applications in various biomedical fields such as sustained and high-efficiency drug delivery.

3.2. The synthesis of yolk–shell Fe_3O_4@PMAA composite microspheres

The magnetic and tunable porous yolk–shell was synthesized for the first time as a drug delivery system. In the first step,

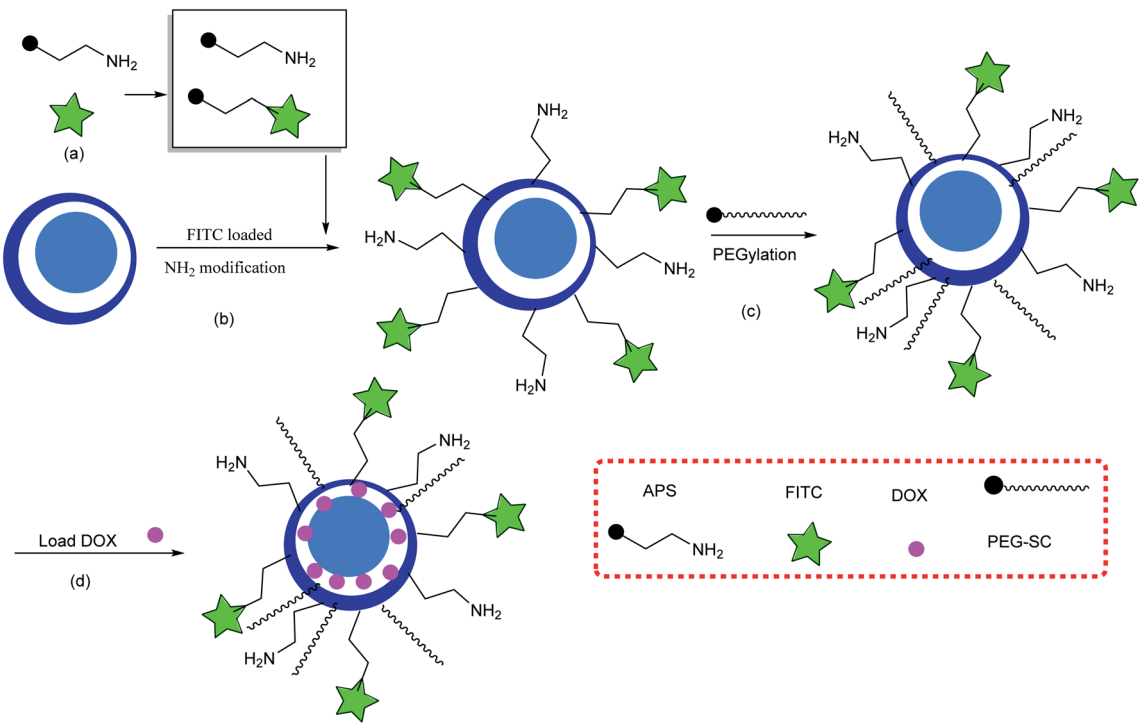

Scheme 2 FITC- and PEG-modified SYSNs. (a) Preparing APS and a conjugated APS–FITC mixture, (b) loading FITC and amino groups on the surface of the SYSN, and (c) PEG-functionalized SYSNs, and (d) loading DOX.

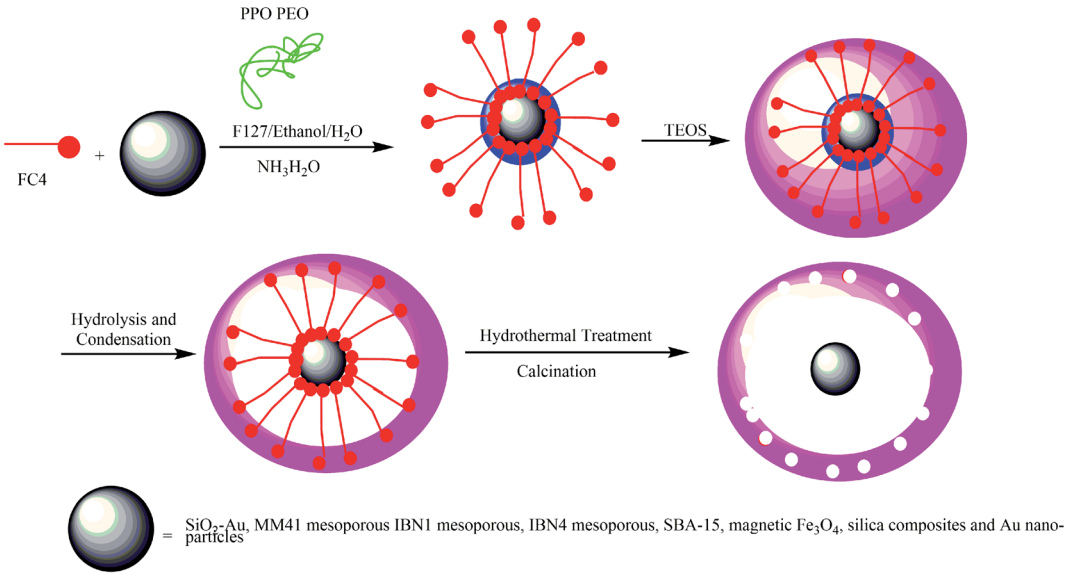

Scheme 3 The synthesis of a yolk–shell–yolk–shell structure with a mesoporous shell.

monodispersed Fe_3O_4 nanoparticles were prepared and then coated by TEOS to provide Fe_3O_4@SiO_2 nanoparticles, which were polymerized with methyl methacrylate (MMA) to produce Fe_3O_4@SiO_2@PMMA with both high magnetization and pH-responsive properties. In the final step, the interlayer silica was removed by adding NaOH, while polymethyl methacrylate (PMMA) was hydrolyzed to hydrophilic polymethacrylic acid (PMAA), and yolk–shell Fe_3O_4@PMAA composite microspheres were subsequently produced (Scheme 6).[49] The microspheres were used for the first time to absorb heavy metals. Ceftriaxone sodium (CTX), a water-soluble anti-inflammatory drug, was selected as a model drug for investigation of loading and controlling in drug delivery.[50] PMAA, which is a pH-responsive polymer, has been applied as a drug-releasing control and is also used in high-capacity drug loading because of the vacant space in its structure.

3.3. The synthesis of yolk–shell Fe_3O_4@PFH@PMAA microspheres

Yolk–shell Fe_3O_4@PFH@PMAA-DOX microspheres were synthesized as a biodegradable carrier for controlled drug delivery. In the synthetic procedure to prepare yolk–shell Fe_3O_4@PFH@PMAA-DOX, Fe_3O_4 was synthesized using $FeCl_3 \cdot 6H_2O$ as a precursor, poly(γ-glutamic acid) (PGA) as a stabilization agent, and ethylene glycol as a reducing agent. Then, the core–shell Fe_3O_4@u-PMAA microspheres were prepared by adding poly(methacrylic acid) (MAA) in the presence of 2,2-azobis-isobutyronitrile (AIBN). In the next step, Fe_3O_4@u-PMAA was coated by disulfide-crosslinked PMAA (d-PMAA), and then, BACy, MAA, and AIBN were added to Fe_3O_4@u-PMAA and Fe_3O_4@u-PMAA@d-PMAA. Finally, the yolk–shell Fe_3O_4@PMAA microspheres were obtained by dispersing Fe_3O_4@u-PMAA@d-PMAA in ethanol to remove uncrosslinked PMAA cores (Scheme 7).[51] Anticancer drug DOX was chosen as a model drug to investigate the drug loading and controlled release behavior. After loading DOX, perfluorohexane (PFH), which is an acoustically sensitive agent, was loaded in the inner cavities and is noted as Fe_3O_4@PFH@PMAA–DOX. Ultrasound energy induced PFH to form into small bubbles, which enhanced the ultrasound signal and increased the permeability of the vessel. After being injected into nude mice with pancreatic cancer, it was found that the mice died after 72 h. Thus, the yolk–shell Fe_3O_4@PFH@PMAA–DOX microspheres were suitable for actual clinical applications.

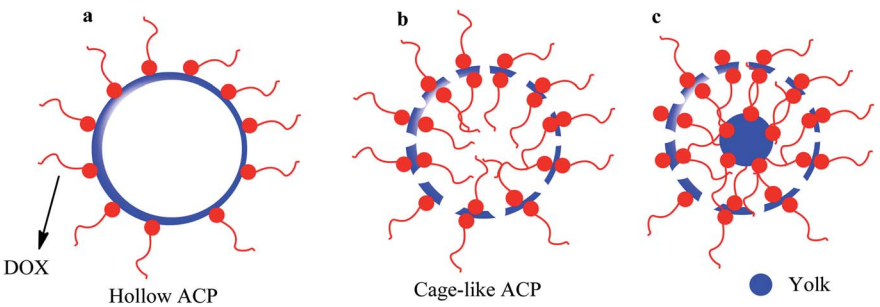

Scheme 4 Loading of DOX molecules on (a) hollow spherical ACP nanoparticles without a cavity, (b) cage–shell hollow spherical ACP nanoparticles, and (c) yolk@cage–shell hollow spherical ACP nanoparticles.

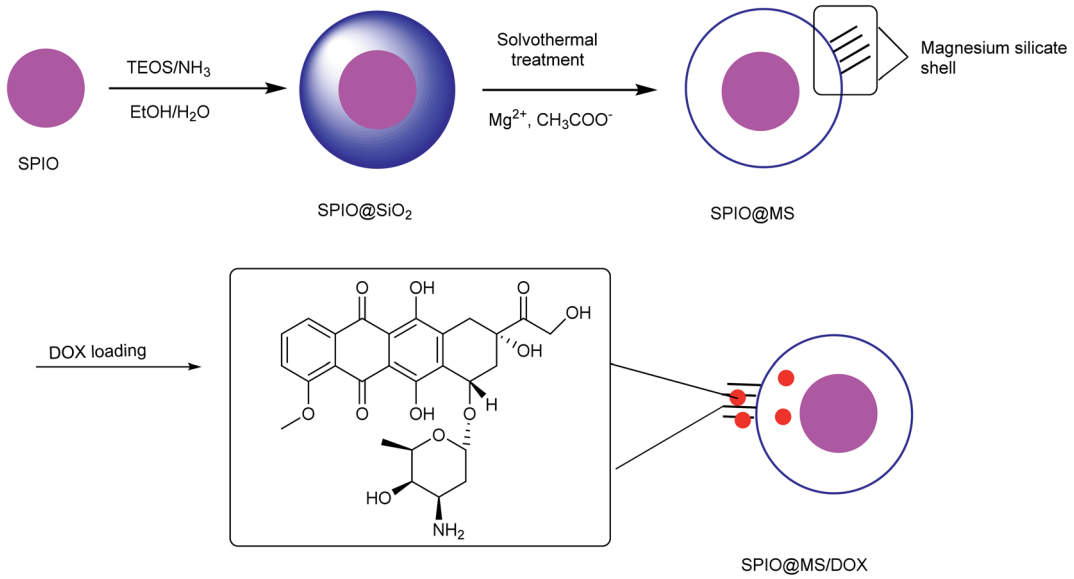

Scheme 5 The synthesis of yolk–shell porous iron oxide@magnesium silicate nanospheres.

3.4. The synthesis of $MnFe_2O_4$@dSiO_2@mSiO_2 yolk–shell

A smart yolk–shell nanocomposite was prepared with an encapsulated Yb(III) complex as a drug delivery carrier. For this purpose, highly uniform $MnFe_2O_4$ was synthesized by a thermal decomposition method in the presence of $ZnCl_2$, $MnCl_2$, $Fe(acac)_3$, oleic acid, oleylamine, and phenylate as a solvent. Afterward, $MnFe_2O_4$ was added to a solution of cyclohexane and poly(oxyethylene)nonyl phenyl ether, and NH_4OH and TEOS were added to the solution at different times to produce $MnFe_2O_4$@uniform dense silica (dSiO_2). The prepared $MnFe_2O_4$@dSiO_2 was added to a mixture containing ethanol, water, CTAB, NH_4OH, TEOS, phenyltriethoxysilane (PTES), (3-aminopropyl)triethoxysilane (APTES) and 2-thenoyltrifluoroacetone–Si (TTA–Si) was then dropped into the reaction mixture to produce $MnFe_2O_4$@dSiO_2@mSiO_2. Finally, the $MnFe_2O_4$@uniform dense silica (dSiO_2)@mesoporous silica shell (mSiO_2) was treated with Na_2CO_3 to provide $MnFe_2O_4$@dSiO_2@mSiO_2 yolk–shell (Scheme 8).[52] YbL(TTA)$_3$, DOX, and carboxymethyl chitosan (cCTS) were each encapsulated in the $MnFe_2O_4$@dSiO_2@mSiO_2 yolk–shell, and then, $MnFe_2O_4$@HMSN@YbL(TTA)@DOX@cCTS was successfully prepared. It was used for tumor-targeted therapies, and the pharmacokinetics were studied so that we could determine the most effective administration of the drug.

3.5. The synthesis of yolk–shell MHMS

MHMS nanospheres were prepared as drug carriers by reaction between iron oxide nanoparticles Fe_3O_4, positively charged CTAB, and polystyrene (PS) nanospheres. The PS nanospheres were synthesized through a co-precipitation method to form the original emulsion template A through self-assembly interaction, and the spheres were coated by TEOS and fixed with Fe_3O_4 nanoparticles to provide B. In this process, the preliminary mesoporous structure was designed to consist of a CTAB/silica nanocomposite, and the PS nanospheres with Fe_3O_4 nanoparticles added on the surface were covered by the silica shell. Finally, model B was deleted, and Fe_3O_4 nanoparticles were placed into the hollow cavity (Scheme 9).[53] The yolk–shell MHMS nanospheres were prepared and applied as an enrofloxacin hydrochloride carrier through a vacuum-recrystallization process. The obtained results exhibit low cytotoxicity, satisfactory biocompatibility and drug release, and high drug-loading capacity for yolk–shell MHMS nanospheres, which make them suitable for medical use.

3.6. The synthesis of Fe_3O_4@graphene yolk–shell

Magnetic and pH-sensitive yolk–shell hybrid nanoparticles were prepared through the reaction of graphene oxide, NaAc, and $FeCl_3$ to synthesize core–shell Fe_3O_4@graphene

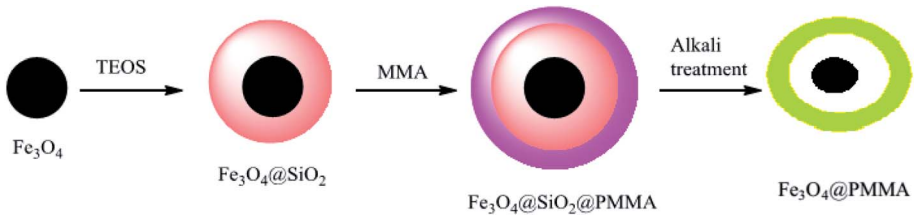

Scheme 6 The synthesis of yolk–shell Fe_3O_4@PMAA composite microspheres.

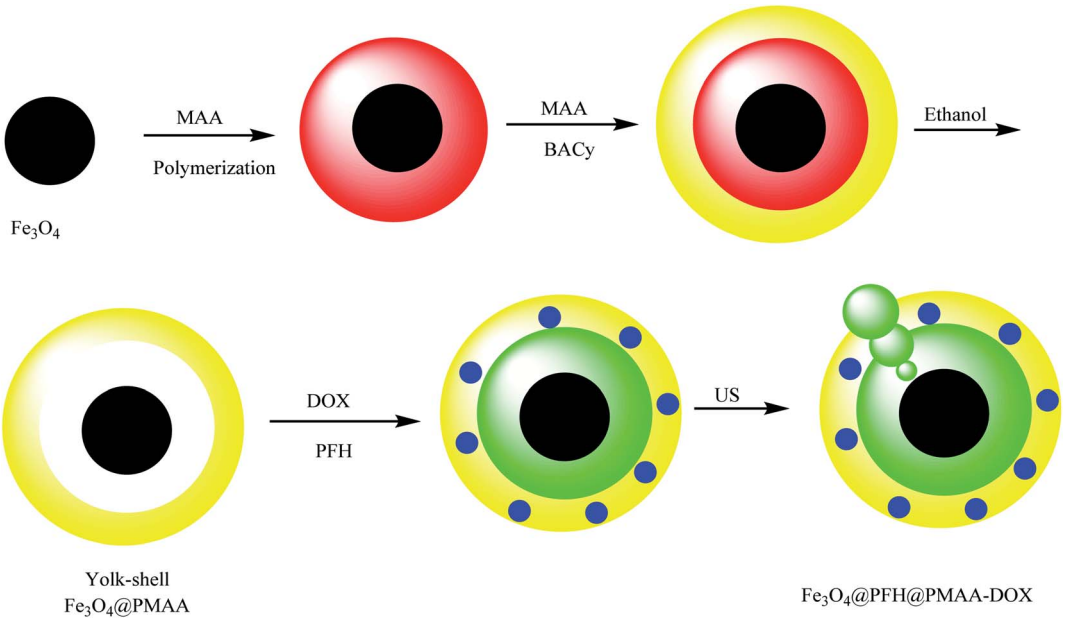

Scheme 7 The synthesis of yolk–shell Fe_3O_4@PFH@PMAA microspheres.

nanoparticles, which were converted to the yolk–shell–yolk–shell form by adding HCl (Scheme 10).[54] DOX was chosen as a model drug for the drug release investigation of the Fe_3O_4@graphene yolk–shell, which was demonstrated to possess a high capacity of loading and biocompatibility for drug delivery applications.

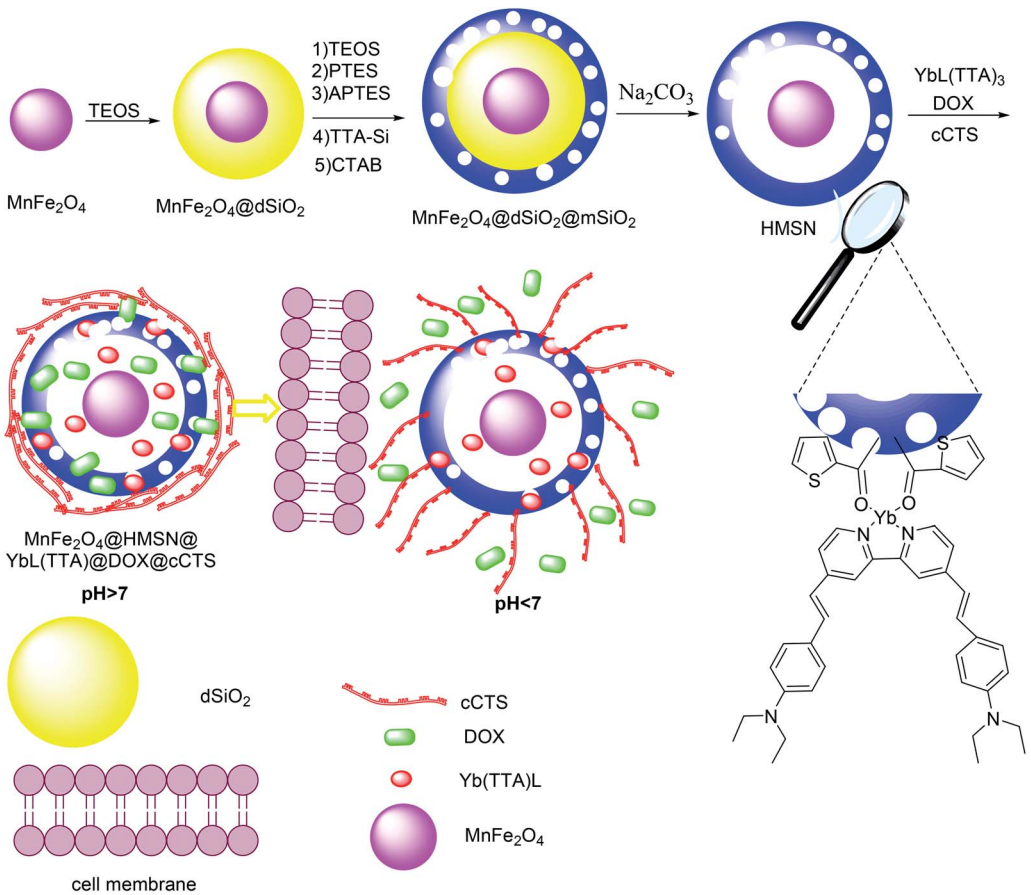

Scheme 8 The synthesis of $MnFe_2O_4$@$dSiO_2$@$mSiO_2$ yolk–shell.

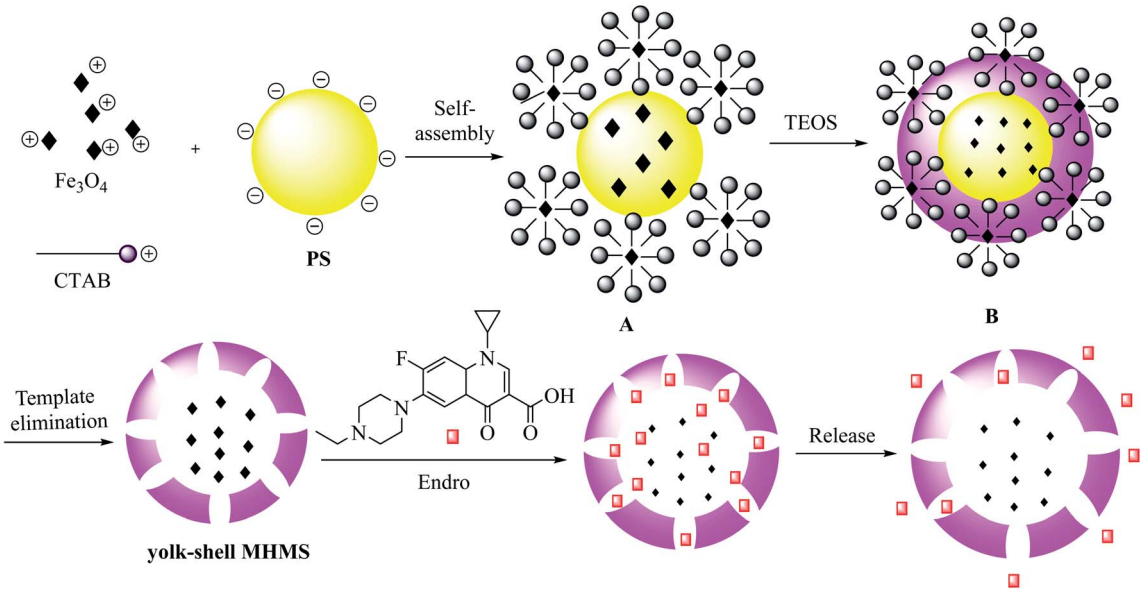

Scheme 9 The synthesis of yolk–shell MHMS.

3.7. The synthesis of nanostar-shaped mesoporous silica

Nanostar-shaped mesoporous silica was fabricated through the addition of CTAT, AHMPD, and deionized water to the reaction mixture, which was mechanically stirred for 1 h. After that, TEOS was quickly injected into the reaction mixture, and after the solution was stirred for 2 h, the nanostars were produced and were subsequently collected by filtration. Magnetic nanostars were synthesized *via* an electrostatic process along with a soft-templating process, as shown in Scheme 11a. AHMPD, a water-based ferrofluid (Fe_3O_4/water), and deionized water were mixed, stirred for 10 min, and then, the particles in the solution were allowed to settle. TEOS was added dropwise to the reaction mixture, which was stirred for 50 min to form the core structure. Then, CTAT was added to obtain soft-templating conditions for 1 h. After that, TEOS was quickly injected into the reactor, and the solution was stirred for 2 h to provide magnetic nanostars. In this way, three types of magnetic nanostars (MNS), namely M_2NS, $M_{1.5}NS$, and M_1NS, were synthesized by adding different amounts of water-based ferrofluid.

Bifunctionalized nanostars and magnetic nanostars were synthesized *via* out-inside bifunctionalization technology. First, dried β-CD[55,56] was reacted with the N=C=O bonds of (3-isocyanatopropyl)triethoxysilane (IPTS), and the solution was stirred for 72 h to obtain Si–β-CD, as shown in Scheme 11b. To the dried nanostars or magnetic nanostars with a template (containing 1.0 g of pure SiO_2), KH590/xylene was added, and the solution was then refluxed for 24 h, and filtered to obtain a powder. The templates were removed from all types of nanostars by adding a solution of NH_4NO_3/ethanol and stirring for 3 h. Then, different amounts of Si–β-CD in xylene/DMF solution were added to the reaction

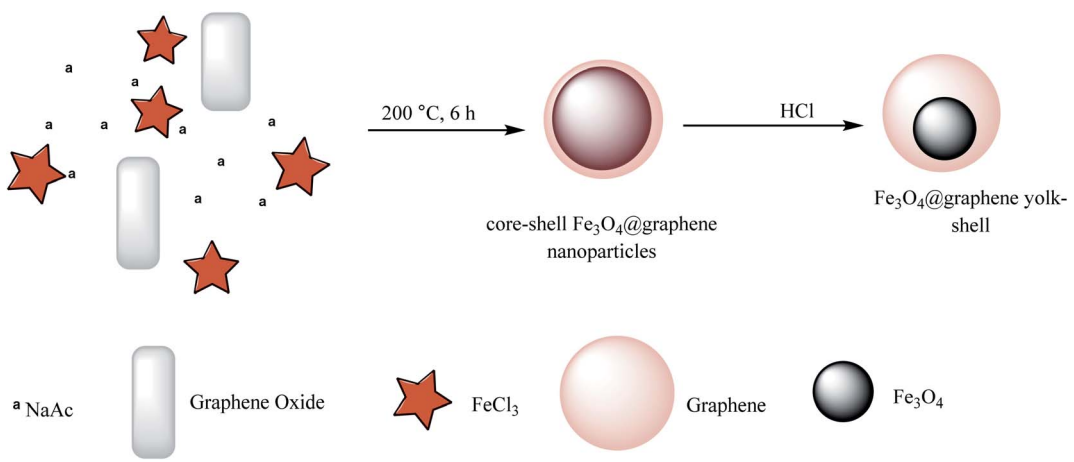

Scheme 10 The synthesis of Fe_3O_4@graphene yolk–shell.

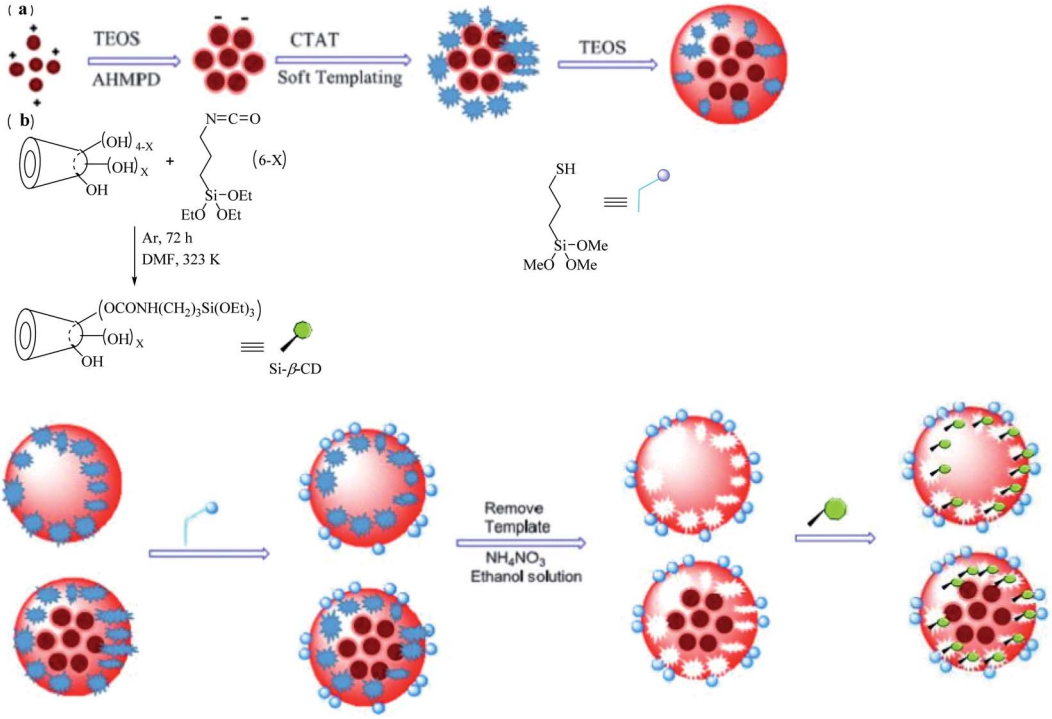

Scheme 11 The synthesis of (a) magnetic nanostars (MNS) and (b) a nanostar form drug delivery system with two functional groups.

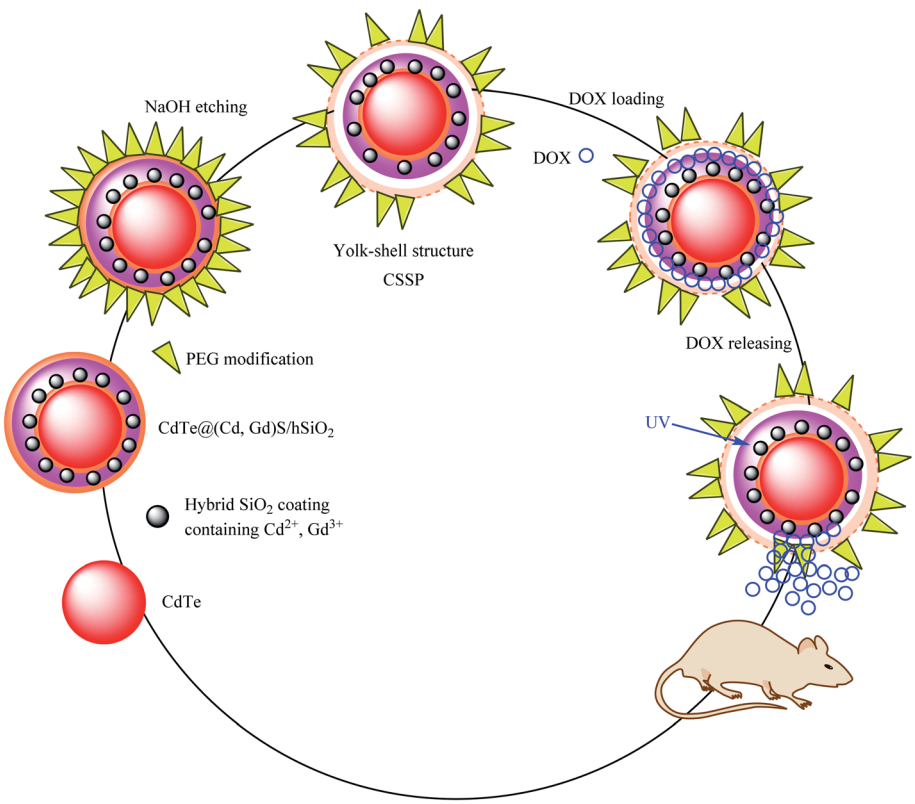

Scheme 12 The synthesis of a CdTe@(Cd,Gd)S/mhSiO_2–PEG (CSSP) yolk–shell.

mixture, which was refluxed for 24 h to form different bifunctionalized nanostars.[56]

3.8. The synthesis of CdTe@(Cd,Gd)S/mhSiO$_2$-PEG (CSSP) yolk–shell

Multifunctional diagnostic nanoplatform core–shell–shell nanosphere (CSSP) structures are provided as a permeable yolk–shell and a potential nanoscale multimodal visible delivery system. In the CSSP yolk–shell synthesis, at the first step, CdTe acts as the core. CdTe was modified by a thin SiO_2 layer containing Cd^{2+} and Gd^{3+} to obtain CdTe@(Cd,Gd)S/mhSiO$_2$, which was added to poly(ethylene glycol) (PEG) to provide CdTe@(Cd,Gd)S/hSiO$_2$-PEG. In the final step, the SiO_2 shell was etched by adding sodium hydroxide to obtain CdTe@(Cd,Gd)S/mhSiO$_2$-PEG (CSSP) yolk–shell nanoparticles, which were dispersed in deionized water at room temperature. Due to the unpaired electron and high spin magnetic moment of the Gd^{3+} ions, this structure can be used in magnetic resonance imaging (MRI) through the coordination of Gd^{3+} with organic ligands. The DOX drug was chosen as a model and loaded on CSSP to obtain SSP–DOX, which was shown to be more capable of killing cancer cells *in vitro* than free DOX (Scheme 12).[57] The release studies were performed in phosphate-buffered saline (PBS) at different pH values (pH 5.0 and 7.4). The amount of released DOX in the supernatant was quantified by UV-Vis spectrophotometry at 490 nm based on the Beer–Lambert law.

3.9. The synthesis of AuNR@PAA/CaP yolk–shell NPs

For the synthesis of AuNR@PAA/CaP yolk–shell NPs, with the first auric nanorod (AuNR) as a yolk, $HAuCl_4$ and CTAB were mixed in a $NaBH_4$ solution in an ice bath to prepare AuNRs. The AuNRs were coated with TEOS to produce AuNR@mSiO$_2$ core–shell nanoparticles. The resulting nanoparticles were added to a solution of $Ca(OH)_2$ and polyacrylic acid (PAA) to obtain polyacrylic acid/calcium ((PAA)/Ca) as a shell, which was mixed with isopropyl alcohol (IPA) and Na_2HPO_4 and etching mesoporous silica shell layer AuNR@mSiO$_2$NPs to provide AuNR@PAA/CaP yolk–shell NPs (Scheme 13).[58] DOX was loaded

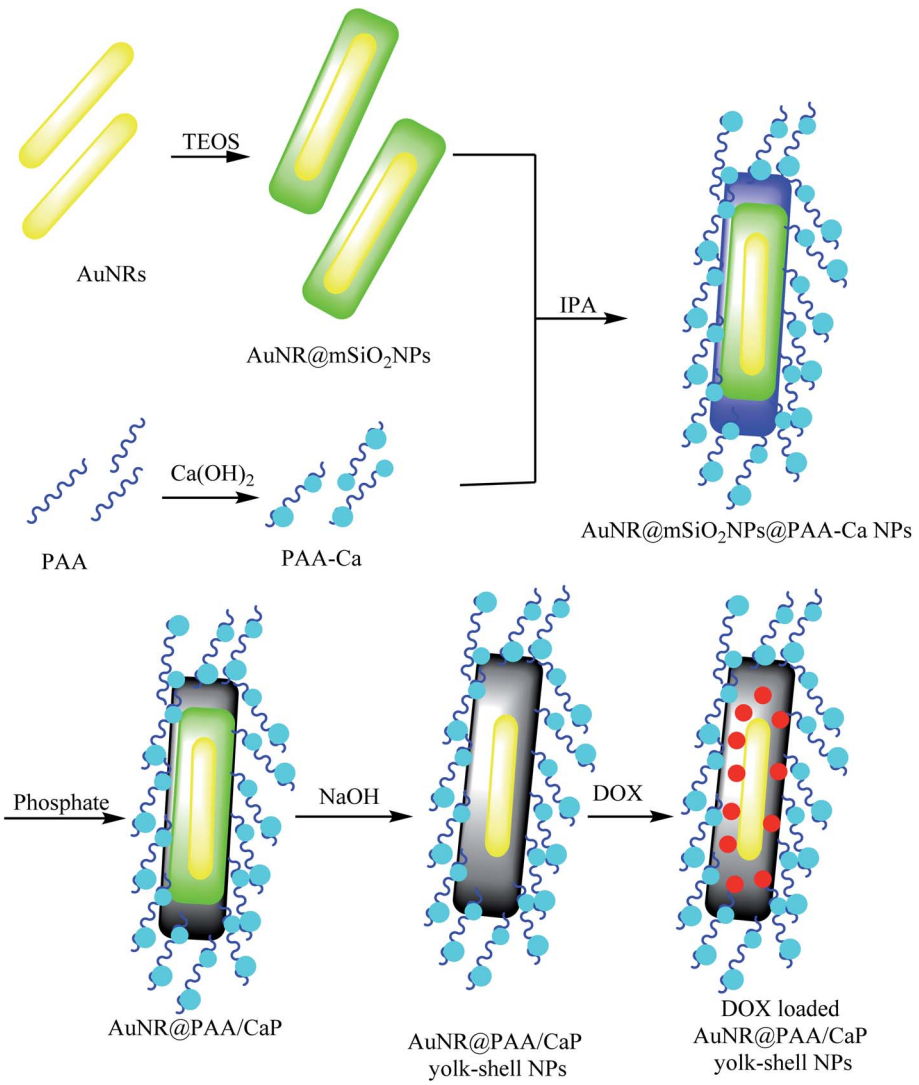

Scheme 13 The synthesis of AuNR@PAA/CaP yolk–shell NPs.

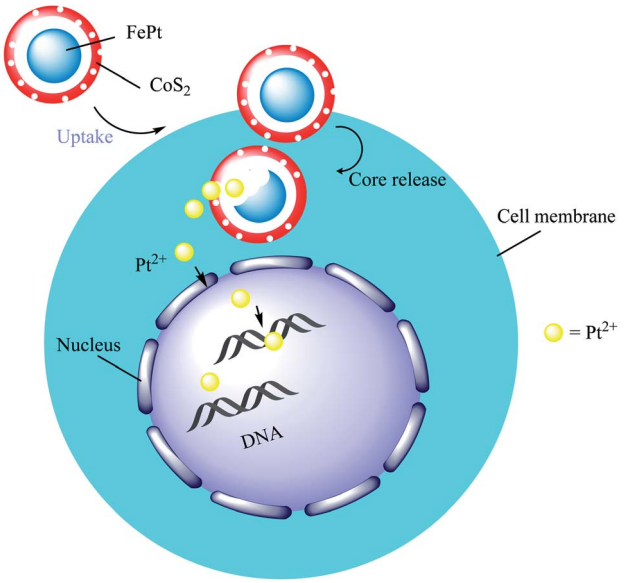

Scheme 14 The synthesis of FePt@CoS_2 yolk–shell nanocrystals and the mechanism used for killing HeLa cancer cells.

as a model drug in the AuNR@PAA/CaP yolk–shell NPs, which exhibited a significant loading efficiency of DOX molecules of approximately 100% due to high a void space. The loading content was 1 mg of the yolk–shell NPs.

3.10. The synthesis of FePt@CoS_2 yolk–shell nanocrystals

In this study, FePt@CoS_2 yolk–shell nanocrystals were developed by Gao and co-workers. For preparing FePt nanoparticles as the core, $Co_2(CO)_8$ in 1,2-dichlorobenzene solution was added to oleic acid, FePt nanoparticles, and trioctylphosphine oxide (TOPO) surfactant solution to produce the FePt@Co core–shell. In the final step, sulfur was added to the FePt@Co core–shell to give FePt@CoS_2 yolk–shell nanocrystals (Scheme 14).[22] In this structure, cobalt atoms diffuse to other layers to form the void. The presence of this void and the binding of Pt ions to DNA indicated that this structure would be ideal as a carrier for Pt, which is a nanomedicine candidate for treating cancer and killing HeLa cancer cells. After cellular uptake, FePt nanoparticles were oxidized to give Fe^{3+} (omitted in Scheme 14 for clarity) and Pt^{2+} ions (yellow). The Pt^{2+} ions enter into the nucleus (and mitochondria), bind to DNA, and lead to apoptosis of the HeLa cancer cells.

3.11. The synthesis of Au yolk/layered double hydroxide (LDH) shell nanoparticles

Au yolk–LDH shell nanoparticles were prepared with Au–cit NPs using a seeded growth strategy. Then, the anticancer drug methotrexate (MTX) was coupled with Au nanoparticles to prepare Au–MTX. Afterward, TEOS was added to prepare the Au–SiO_2 core–shell. Finally, a mixed solution containing Mg^{2+}, Al^{3+}, and MTX was added to the Au@SiO_2 system under a suitable pH value to fabricate the Au@LDH–MTX structure (Scheme 15).[59] Investigation showed that Au@LDH–MTX is more effective at breast cancer inhibition than free MTX.

4. Synthesis and application of polymer core-based yolk/shell structures

4.1. The synthesis of CPMAA@CPNIPAM yolk/shell and RS-CPMAA@CPNIPAM yolk/shell microspheres

In this study, the polymerization reaction of methacrylic acid (MAA) as the monomer, ethyleneglycol dimethacrylate (EGDMA) as the crosslinker, and AIBN as initiator provided crosslinked poly(methacrylic acid) (CPMAA) nanoparticles. CPMAA cores were dispersed into water, and then, *N*-isopropyl acrylamide (NIPAM), sodium dodecylbenzene sulfonate (SDS), and ammonium persulfate (APS) were added to obtain CPMAA@poly *N*-isopropylacrylamide (PNIPAM), as shown in Scheme 16. Then, the resulting product was added to NIPAM, divinyl benzene (DVB), and APS to provide CPMAA@PNIPAM@CPNIPAM microspheres by polymerization. Finally, raspberry-shaped CPMAA@CPNIPAM yolk–shell was synthesized by self-removal. An approach was based on consecutive radical seeded (RS) emulsion copolymerization by water.[60] Regular CPMAA@CPNIPAM core/shell microspheres were prepared for comparison with RS-CPMAA@CPNIPAM yolk/shell microspheres regarding drug-loading capacity. DOX-loaded

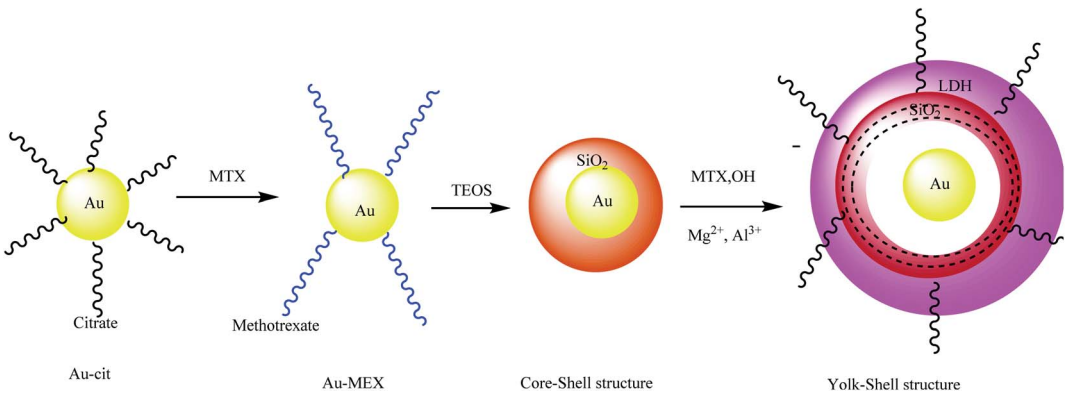

Scheme 15 The synthesis of Au yolk/LDH shell nanoparticles.

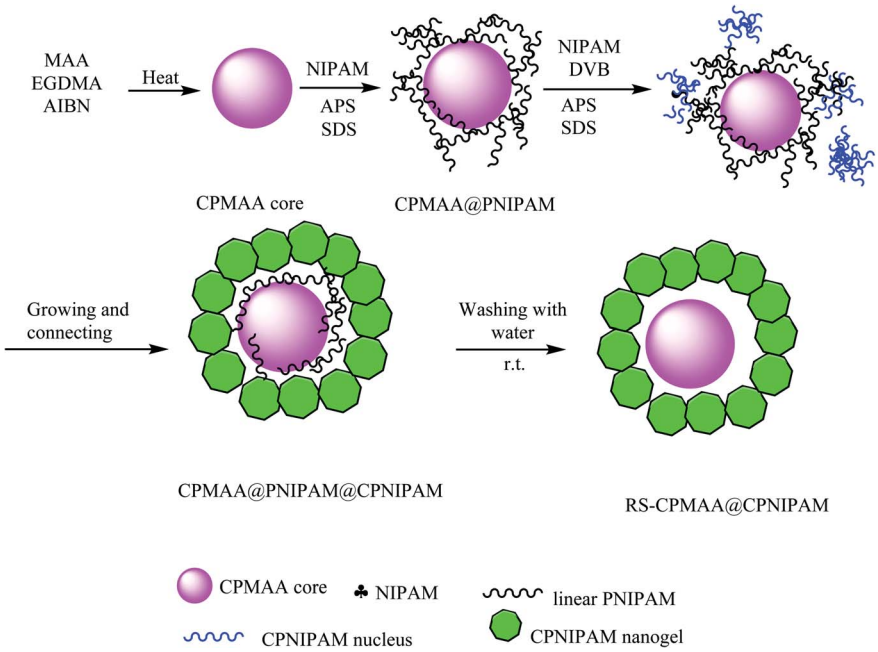

Scheme 16 The synthesis of CPMAA@CPNIPAM yolk/shell and the RS-CPMAA@CPNIPAM yolk/shell microspheres.

Table 1 Drug loading capacity of the two drug carriers in media with different pH values

	Drug loading capacity (%)		
Drug carriers	pH 7.4	pH 6.5	pH 5.0
CPMAA@CPNIPAM	10.2	8.2	7.5
RS-CPMAA@CPNIPAM	35.4	12.0	10.0

microspheres were used for detecting DOX concentration in supernatant liquid with a UV-Vis spectrophotometer, as summarized in Table 1. The results showed that the drug-loading capacity of the RS-PMAA@CPNIPAM yolk–shell microspheres was higher than that of the CPMAA@PNIPAM core/shell microspheres in all three cases.

4.2. The synthesis of yolk/shell PMAA/PNIPAM microspheres

Liu and co-workers synthesized yolk/shell PMAA/poly *N*-isopropylacrylamide (PNIPAM) microspheres to be dual-stimuli responsive yolk–shell polymers that are independent of temperature and pH. The synthetic method of this yolk–shell micro-hollow is as follows: MAA was polymerized to prepare polymethacrylic acid (PMAA) and then coated with TEOS to provide PMAA@SiO_2, which was stabilized by adding 3-(methacryloxy)propyl trimethoxysilane (MPS) on the surface of the PMAA@SiO_2 microspheres. In the next step, the PMAA@SiO_2@PNIPAM microspheres were prepared by precipitation polymerization of *N*-isopropyl acrylamide (NIPAM) and *N*,*N*′-methylene bisacrylamide (MBA) on the PMAA/SiO_2 microspheres as seeds. In the final stage, the resultant sandwich consisting of PMAA@SiO_2@PNIPAM microspheres was dispersed in aqueous hydrofluoric (HF) acid solution for etching the silica interlayer to obtain the yolk–shell PMAA@PNIPAM microspheres (Scheme 17).[61] DOX was used as the model drug to investigate drug-loading capacity under *in vitro* conditions because the cavity diameters and the lower PNIPAM crosslinking degree played a slight role in the drug-loading capacity and controlled release of yolk–shell PMAA@PNIPAM microspheres.

4.3. The synthesis of pH-stimuli P(DEAEMA-styrene)

The copolymer pH-stimuli P(DEAEMA-styrene) (PDS) was produced through a free-radical polymerization of monomers

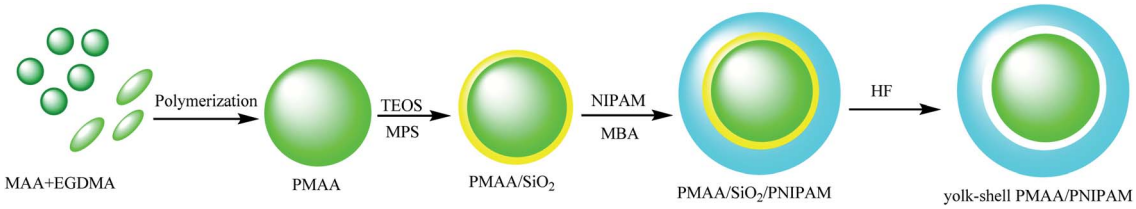

Scheme 17 The synthesis of yolk/shell PMAA/PNIPAM microspheres.

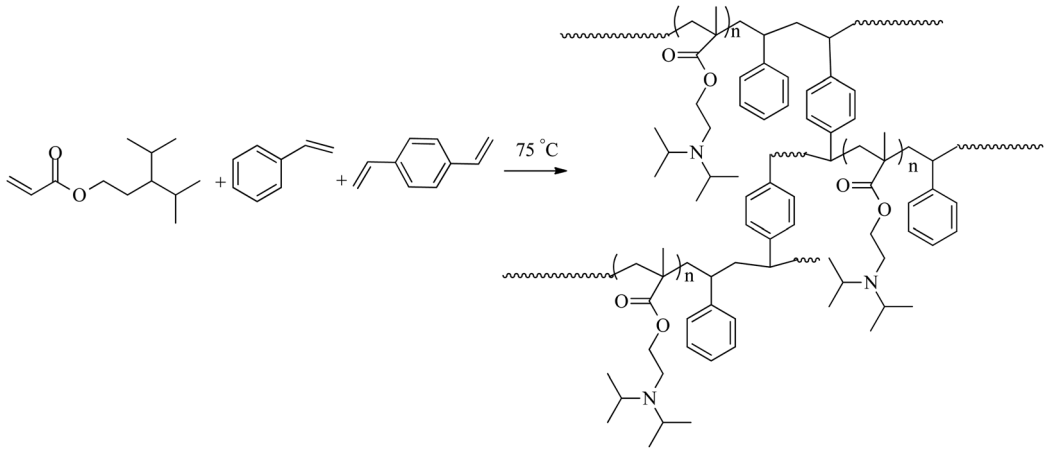

Fig. 1 The synthesis route of pH-stimuli PDS.

styrene (St), 2-(diethylamino)ethyl methacrylate (DEAEMA), divinylbenzene (DVB), and 2,2-azobisisobutyronitrile (AIBN) as the resulting hydrophobic mixture, which was added to a sodium dodecylbenzene sulfonate solution (SDBS) as a yolk (Fig. 1).

A drug-loaded yolk–shell microcapsule was prepared with poly(2-(diethylamino)ethyl methacrylate-styrene) (PDS) as a yolk and polystyrene as a shell. This microcapsule was synthesized by the all-in-one method of solvent evaporation and emulsion polymerization. In this method, polystyrene (PS) as the shell in dichloromethane (DCM), 2-(diethylamino)ethyl methacrylate (DEAEMA), styrene (St), 2,2-azobisisobutyronitrile (AIBN), divinylbenzene (DVB), and ibuprofen (IBU) (drug-loaded in microcapsule) as core materials were mixed. Then, sodium dodecylbenzene sulfonate (SDBS) was added as an emulsifier agent to provide microcapsules, which were applied as carriers for controlled drug release.[62] The ibuprofen drug release results showed that these pH-responsive microcapsules are a capable carrier for drug delivery and pH-responsive environmental bioindicators. The drug release mechanism of the resulting microcapsules is pictured in Scheme 18. In this process, the pH-sensitive tertiary amino parts of PDS were changed into quaternary ammonium cations through changes in pH from 7.5 to 5.3. The hydrophobic PDS converted to hydrophile ones in which the volume of PDS increased *via* decreasing the pH to 3.4 by protonation. Because the pH-responsive structure of PDS extensively widens, the volume of PDS greatly increased. The microcapsule cavity was in the hydrophilic form, resulting in expulsion and diffusion of the drug.

4.4. The synthesis of P(MAA-*co*-EGDMA)/SiO_2/PNIPAM sandwich microspheres

In this method, microgel poly(methacrylic acid-*co*-ethyleneglycol methacrylate) (P(MAA-*co*-EGDMA)) cores were obtained *via* the facile distillation precipitation copolymerization of ethylene glycol dimethacrylate (EGDMA), methacrylic acid (MAA), and AIBN as the initiator in acetonitrile. In the next step,

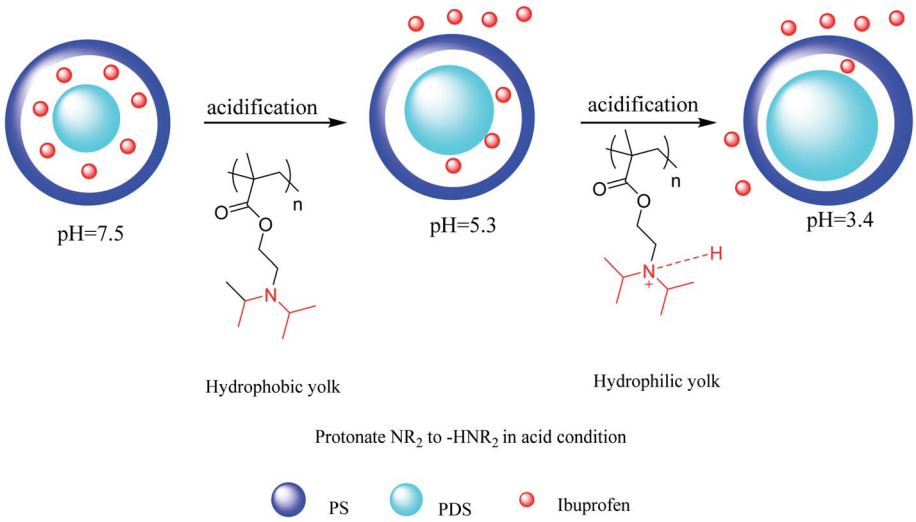

Scheme 18 An illustration of the drug release mechanism by yolk swelling through decreasing pH values.

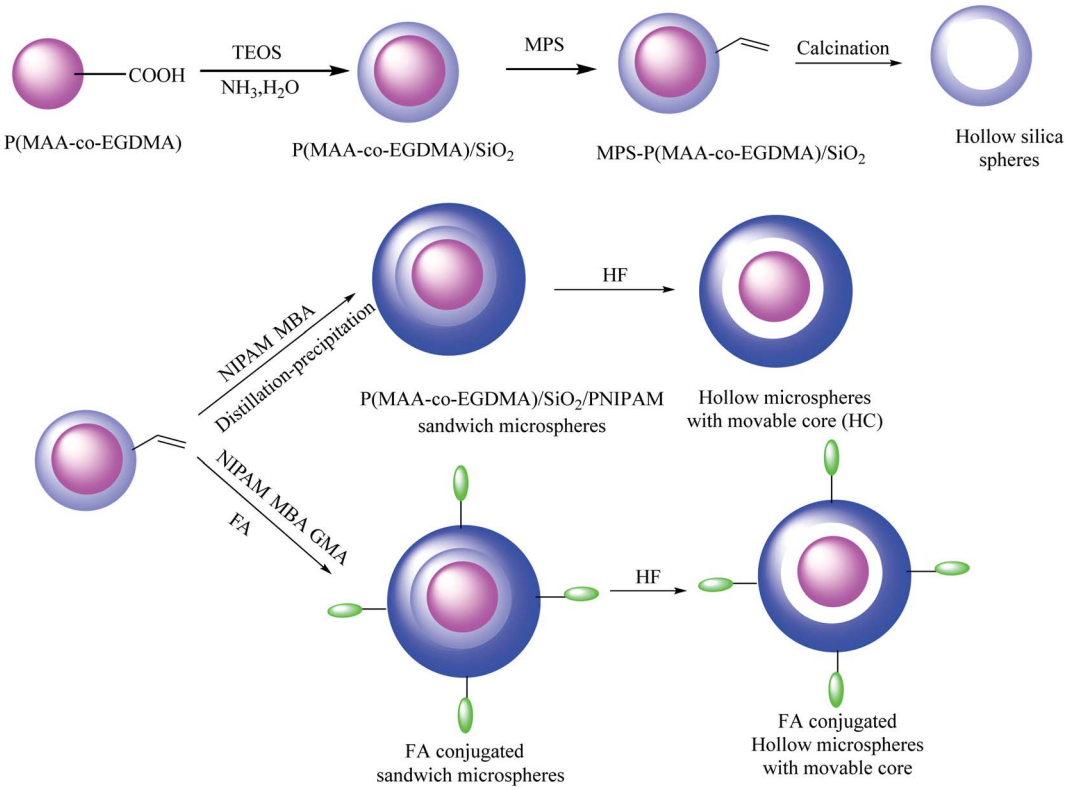

Scheme 19 The synthesis of P(MAA-*co*-EGDMA)/SiO_2/PNIPAM sandwich microspheres.

(P(MAA-*co*-EGDMA)@SiO_2) core@shell was synthesized by the application of an outer silica layer coating onto the P(MAA-*co*-EGDMA) microgels *via* the sol–gel process. P(MAA-*co*-EGDMA)@SiO_2 was modified with MPS to incorporate the reactive vinyl groups and prepare MPS-modified P(MAA-*co*-EGDMA)@SiO_2 core–shell. Hollow silica microspheres were obtained by selective removal of the P(MAA-*co*-EGDMA) microgel cores in the P(MAA-*co*-EGDMA)@SiO_2 core–shell microspheres during calcination. The resulting MPS-modified P(MAA-*co*-EGDMA)@SiO_2 core–shell was coated with poly(*N*-isopropyl acrylamide) (PNIPAM) to provide P(MAA-*co*-EGDMA)@SiO_2@PNIPAM sandwich microspheres. For preparing folic acid-conjugated P(MAA-*co*-EGDMA)@SiO_2@PNIPAM sandwich microspheres, the P(MAA-*co*-EGDMA)@SiO_2@PNIPAM sandwich microspheres were functionalized with glycidyl methacrylate (GMA) monomer, and then, the resultant materials were added to folic acid (FA) solution. Finally, the silica shell was removed by adding hydrofluoric (HF) acid to synthesize pH- and temperature-responsive yolk–shell microspheres (Scheme 19).[63] DOX was selected as a model drug for investigating the drug

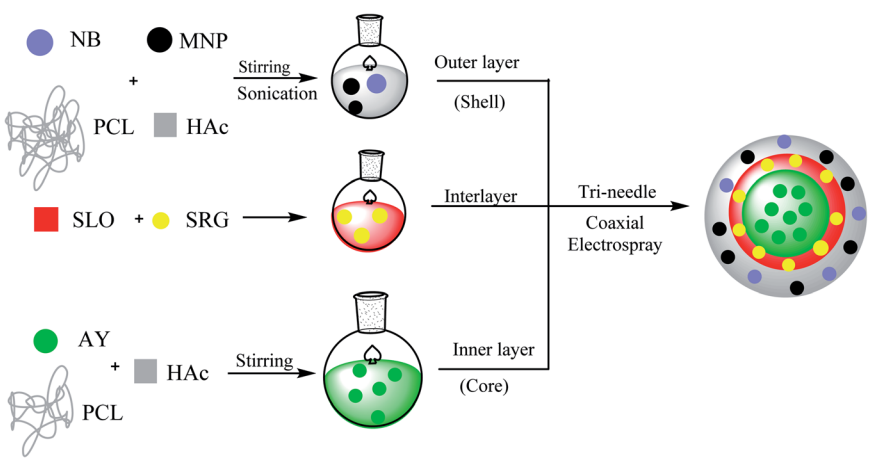

Scheme 20 The synthesis of magnetic polymer yolk–shell particles.

delivery capability of this yolk–shell structure. According to the observed results, the remarkable addition was revealed in drug-loading capacity at pH 7.4 due to the cavity of the hollow microspheres and the polymethacrylic acid (PMAA) cores, which were located inside the hollow microspheres and were able to interact with the DOX molecules.

4.5. The synthesis of magnetic polymer yolk–shell particles

Magnetic polymer yolk–shell particles were engineered by poly(ε-caprolactone) (PCL) as the matrix for core and shell parts, which were permeable for drug delivery. Additionally, silicone oil (SLO) was adopted for use with PCL due to its viscosity.[64,65] In this study, Nile blue (NB) and acridine yellow (AY) were selected as hydrophilic probes. To provide the magnetic properties, Fe_3O_4 magnetic nanoparticles (MNs) were encapsulated into yolk–shell particles (YSPs). The magnetic polymer yolk–shell particles were synthesized in a single-step tri-needle coaxial electrospraying process. In this process, an outer layer, interlayer, and inner layer were created through the tri-needle coaxial electrospraying method. A mixture of PCL, Nile blue (NB), glacial acetic acid (HAc), and MNPs Fe_3O_4 was used to construct the outer layer. Silicone oil (SLO) and Sudan red G (SRG) were injected as an interlayer. The inner layer as the core was obtained through the mixing of PCL, AY, and HAc. All layers were fabricated using different flow rates to release the hydrophobic and hydrophilic agents. Furthermore, NB and AY were selected as hydrophilic agents to load on the external shell and inner core, respectively. SRG was loaded as a hydrophobic agent on the silicone oil layer (Scheme 20).[66] The experimental results showed that these structures have promising applications in multi-drug dosing therapy due to their suitable effects, which were observed *via* the process of encapsulation of hydrophobic and hydrophilic agents.

5. Conclusion

Yolk–shell nanoparticles (YSNPs) are a unique class of nanomaterials with tunable physical and chemical properties. In this study, numerous methods were summarized that describe the synthesis of different yolk–shell structures with many yolks and shells. Furthermore, their applications in drug delivery systems were studied. Their movable cores with cavities and hollow shells provided highly significant drug carriers. Cancer therapy medicines are the most commonly used drugs for encapsulation as YSNPs, which can protect organs from a toxic drug before reaching its target.

Abbreviations

AIBN	2,2-Azobisisobutyronitrile
AHMPD	Tris(hydroxymethyl)aminomethane
APS	Ammonium persulfate
AY	Acridine yellow
AuNRs	Auric nanorods
ACP	Amorphous calcium phosphate
BACy	*N*,*N*-Bis(acryloyl)cystamine
β-CD	Si–β-cyclodextrin
CTX	Ceftriaxone sodium
CTAT	Hexadecyltrimethylammonium toluene-*p*-sulphonate
CdTe	Cadmium telluride
CaP	Calcium phosphate
Cit	Citrate
CTAB	Cetyltrimethylammonium bromide
CSSNs	Core–shell–shell nanospheres
DVB	Divinyl benzene
DOX	Doxorubicin hydrochloride
DCM	Dichloromethane
DEAEMA	2-(Diethylamino)ethylmethacrylate
F127	Triblock copolymer EO106PO70EO106
FC4	Fluorocarbon surfactant
$FeCl_3$	Iron(III) chloride
FA	Folic acid
FITC	Fluorescein isothiocyanate
GAA	Glacial acetic acid
GMA	Glycidyl methacrylate
HCl	Hydrogen chloride
HF	Hydrofluoric acid
IBU	Ibuprofen
IPA	Isopropyl alcohol
KH590	3-Mercaptopropyl-trimethoxysilane
LDH	Layered double hydroxides
MHMS	Magnetic hollow mesoporous silica
MMA	Methyl methacrylate
$MnFe_2O_4$	Manganese iron oxide
MTX	Methotrexate
MNS	Magnetic nanostars
MPS	3-(Methacryloxy)propyl trimethoxysilane
MNPs	Magnetic nanoparticles
NPs	Nanoparticles
NIPAM	*N*-Isopropyl acrylamide
NH_3H_2O	Ammonia-water
NB	Nile blue
NaAc	Sodium acetate
PVP	Polyvinylpyrrolidone
PAA	Polyacrylic acid
PTES	Phenyltriethoxysilane
PSt	Polystyrene
pH	Potential hydrogen
PMAA	Polymethacrylic acid
PGA	Poly(γ-glutamic acid)
PFH	Perfluorohexane
PNIPAM	Poly *N*-isopropylacrylamide
PCL	Poly(ε-caprolactone)
P(MAA-*co*-EGDMA)	Poly(methacrylic acid-*co*-ethyleneglycol dimethacrylate
PEG	Poly(ethylene glycol)
PRs	Phenol-formaldehyde resin spheres
PMMA	Polymethyl methacrylate
QDs	Quantum dots
SPIO	Super paramagnetic iron oxide
SiO_2	Silica
St	Styrene
SDBS	Sodium dodecyl benzene sulfonate
SYSNs	Silica-based yolk–shell nanostructures

SRG	Sudan red G
TGA	Thioglycolic acid
TOPO	Trioctylphosphine oxide
YSNPs	Yolk–shell nanoparticles

Conflicts of interest

There are no conflicts to declare.

Acknowledgements

We are grateful for support from the Research Council of Alzahra University and University of Tehran.

References

1 C. Kinnear, T. L. Moore, L. Rodriguez-Lorenzo, B. Rothen-Rutishauser and A. Petri-Fink, *Chem. Rev.*, 2017, **117**, 11476.
2 V. P. Torchilin, *Pharm. Res.*, 2007, **24**, 1.
3 P. Yang, Z. Quan, C. Li, X. Kang, H. Lian and J. Lin, *Biomaterials*, 2008, **29**, 4341.
4 S. Liu, J. Yu and M. Jaroniec, *J. Am. Chem. Soc.*, 2010, **132**, 11914.
5 R. K. Sharma, S. Dutta, S. Sharma, R. Zboril, R. S. Varma and M. B. Gawande, *Green Chem.*, 2016, **18**, 3184.
6 I. Lee, J. B. Joo, Y. Yin and F. Zaera, *Angew. Chem., Int. Ed.*, 2011, **50**, 10208.
7 S. Rohani, A. Ziarati, G. Mohammadi Ziarani, A. Badiei and T. Bürgi, *Catal. Sci. Technol.*, 2019, **9**, 3820–3827.
8 S. Ding, J. S. Chen, G. Qi, X. Duan, Z. Wang, E. P. Giannelis, L. A. Archer and X. W. Lou, *J. Am. Chem. Soc.*, 2010, **133**, 21.
9 Z. Chen, Z.-M. Cui, F. Niu, L. Jiang and W.-G. Song, *Chem. Commun.*, 2010, **46**, 6524.
10 X. W. Lou, C. M. Li and L. A. Archer, *Adv. Mater.*, 2009, **21**, 2536.
11 M. Retsch, M. Schmelzeisen, H.-J. r. Butt and E. L. Thomas, *Nano Lett.*, 2011, **11**, 1389.
12 G. Li, E. Kang, K. Neoh and X. Yang, *Langmuir*, 2009, **25**, 4361.
13 Y. H. Ng, S. Ikeda, T. Harada, S. Higashida, T. Sakata, H. Mori and M. Matsumura, *Adv. Mater.*, 2007, **19**, 597.
14 X. W. Lou and L. A. Archer, *Adv. Mater.*, 2008, **20**, 1853.
15 P. Valle-Vigón, M. Sevilla and A. B. Fuertes, *Mater. Lett.*, 2010, **64**, 1587.
16 G. Li, Q. Shi, S. Yuan, K. Neoh, E. Kang and X. Yang, *Chem. Mater.*, 2010, **22**, 1309.
17 L. Yu, P. Pan, Y. Zhang, Y. Zhang, L. Wan, X. Cheng and Y. Deng, *Small*, 2019, 1805465.
18 Y. Yu, M. Zhou, W. Zhang, L. Huang, D. Miao, H. Zhu and G. Su, *Mol. Pharm.*, 2019, **16**(5), 1929–1938.
19 Y. A. Nor, H. Zhang, S. Purwajanti, H. Song, A. K. Meka, Y. Wang, N. Mitter, D. Mahony and C. Yu, *J. Mater. Chem. B*, 2016, **4**, 7014.
20 Y. Chen, H. Chen, M. Ma, F. Chen, L. Guo, L. Zhang and J. Shi, *J. Mater. Chem.*, 2011, **21**, 5290.
21 L. Li, D. Qin, X. Yang and G. Liu, *Polym. Chem.*, 2010, **1**, 289.
22 Y.-L. Shi and T. Asefa, *Langmuir*, 2007, **23**, 9455.
23 J. Liu, S. Bai, H. Zhong, C. Li and Q. Yang, *J. Phys. Chem. C*, 2009, **114**, 953.
24 X. W. Lou, C. Yuan, Q. Zhang and L. A. Archer, *Angew. Chem., Int. Ed.*, 2006, **45**, 3825.
25 X. W. Lou, C. Yuan, E. Rhoades, Q. Zhang and L. A. Archer, *Adv. Funct. Mater.*, 2006, **16**, 1679.
26 H. Chun Zeng, *Curr. Nanosci.*, 2007, **3**, 177.
27 J. Li and H. C. Zeng, *J. Am. Chem. Soc.*, 2007, **129**, 15839.
28 X. Gong, Y. Yang and S. Huang, *J. Phys. Chem. C*, 2010, **114**, 18073.
29 J. Liu, S. Z. Qiao, J. S. Chen, X. W. D. Lou, X. Xing and G. Q. M. Lu, *Chem. Commun.*, 2011, **47**, 12578.
30 J. Gao, G. Liang, B. Zhang, Y. Kuang, X. Zhang and B. Xu, *J. Am. Chem. Soc.*, 2007, **129**, 1428.
31 A. Li, W. Zhu, C. Li, T. Wang and J. Gong, *Chem. Soc. Rev.*, 2019, **48**, 1874.
32 R. Chenevert, G. Mohammadi Ziarani and M. Dasser, *Heterocycles*, 1999, **51**, 593.
33 F. Mohajer, G. Mohammadi Ziarani and R. Moradi, *Curr. Org. Chem.*, 2020, **24**, 516.
34 G. Mohammadi Ziarani, F. Mohajer and Z. Kheilkordi, *Curr. Org. Synth.*, 2020, **17**(2), 82–90.
35 V. F. Vavsari, G. Mohammadi Ziarani and A. Badiei, *RSC Adv.*, 2015, **5**, 91686.
36 G. Mohammadi Ziarani, M. Malmir, N. Lashgari and A. Badiei, *RSC Adv.*, 2019, **9**, 25094.
37 G. Mohammadi Ziarani, S. Faramarzi, S. Asadi, A. Badiei, R. Bazl and M. Amanlou, *Daru, J. Pharm. Sci.*, 2013, **21**, 3.
38 G. Song, C. Li, J. Hu, R. Zou, K. Xu, L. Han, Q. Wang, J. Yang, Z. Chen and Z. Qin, *J. Mater. Chem.*, 2012, **22**, 17011.
39 W. Stöber, A. Fink and E. Bohn, *J. Colloid Interface Sci.*, 1968, **26**, 62.
40 Q. Cai, Z.-S. Luo, W.-Q. Pang, Y.-W. Fan, X.-H. Chen and F.-Z. Cui, *Chem. Mater.*, 2001, **13**, 258.
41 Y. Han and J. Y. Ying, *Angew. Chem., Int. Ed.*, 2005, **44**, 288.
42 Y. Yang, S. Karmakar, J. Zhang, M. Yu, N. Mitter and C. Yu, *J. Mater. Chem. B*, 2014, **2**, 4929.
43 H. Xu, N. Tong, L. Cui, Y. Lu and H. Gu, *J. Magn. Magn. Mater.*, 2007, **311**, 125.
44 D. G. Duff, A. Baiker and P. P. Edwards, *Langmuir*, 1993, **9**, 2301.
45 J. Kim, J. E. Lee, J. Lee, Y. Jang, S. W. Kim, K. An, J. H. Yu and T. Hyeon, *Angew. Chem., Int. Ed.*, 2006, **45**, 4789.
46 J. Liu, S. Z. Qiao, S. Budi Hartono and G. Q. Lu, *Angew. Chem., Int. Ed.*, 2010, **49**, 4981.
47 S. Huang, C. Li and Q. Xiao, *Nanoscale Res. Lett.*, 2017, **12**, 275.
48 T.-W. Sun, Y.-J. Zhu, F. Chen, C. Qi, B.-Q. Lu, J. Wu, D. Zhou and C.-Q. Zhang, *RSC Adv.*, 2016, **6**, 103399.
49 L. Zhao, H. Liu, F. Wang and L. Zeng, *J. Mater. Chem. A*, 2014, **2**, 7065.
50 L. Li, L. Zhang, S. Xing, T. Wang, S. Luo, X. Zhang, C. Liu, Z. Su and C. Wang, *Small*, 2013, **9**, 825.
51 P. Yang, X. Luo, S. Wang, F. Wang, C. Tang and C. Wang, *Colloids Surf., B*, 2017, **151**, 333.

52 C. Shan, B. Wang, B. Hu, W. Liu and Y. Tang, *J. Photochem. Photobiol., A*, 2018, **355**, 233–241.
53 F. Liu, J. Wang, Q. Cao, H. Deng, G. Shao, D. Y. Deng and W. Zhou, *Chem. Commun.*, 2015, **51**, 2357.
54 S. Li, J. Zheng, D. Chen, Y. Wu, W. Zhang, F. Zheng, J. Cao, H. Ma and Y. Liu, *Nanoscale*, 2013, **5**, 11718.
55 C. Abbehausen, A. L. Formiga, E. Sabadini and I. V. Yoshida, *J. Braz. Chem. Soc.*, 2010, **21**, 1867.
56 P. Huang, B. Zeng, Z. Mai, J. Deng, Y. Fang, W. Huang, H. Zhang, J. Yuan, Y. Wei and W. Zhou, *J. Mater. Chem. B*, 2016, **4**, 46.
57 M.-L. Chen, S.-C. Pang, X.-M. Chen and L. Li, *Talanta*, 2017, **175**, 280.
58 G. Li, Y. Chen, L. Zhang, M. Zhang, S. Li, L. Li, T. Wang and C. Wang, *Nano-Micro Lett.*, 2018, **10**, 7.
59 X. Huo, C. Dai, S. Li and X. Li, *RSC Adv.*, 2015, **5**, 8689.
60 L. Liu, J. Guo and P. Liu, *Ind. Eng. Chem. Res.*, 2016, **55**, 4790.
61 L. Liu, P. Du, X. Zhao, J. Zeng and P. Liu, *Eur. Polym. J.*, 2015, **69**, 540.
62 J. Jia, C. Wang, K. Chen and Y. Yin, *Chem. Eng. J.*, 2017, **327**, 953.
63 P. Du, H. Yang, J. Zeng and P. Liu, *J. Mater. Chem. B*, 2013, **1**, 5298.
64 Y. Cao, B. Wang, Y. Wang and D. Lou, *J. Pharm. Sci.*, 2014, **103**, 3205.
65 G. Yuan, Z. Ding, M. W. Chang, Z. Ahmad and J. S. Li, *Chem. Eng. J.*, 2015, **284**, 963.
66 C. Zhang, Z.-C. Yao, Q. Ding, J. J. Choi, Z. Ahmad, M.-W. Chang and J.-S. Li, *ACS Appl. Mater. Interfaces*, 2017, **9**, 21485.